Supplemental Material

Supplemental Information for: Chronic inflammation promotes skin carcinogenesis in cancer-prone discoid lupus erythematosus.

Supplemental Methods

Animal carcinogenesis studies

In order to test the development of cancer in the context of chronic inflammation associated with discoid lupus, we designed a skin carcinogenesis protocol (Fig. 2A). On the first day, four-eight-week old female MRL/*lpr* and MRL/*n* control mice were shaved on their back and treated with 50 µg 7,12-Dimethylbenzantracene (DMBA). After a week, all mice were treated twice with 6 µg 12-O-Tetradecanoylphorbol-13-acetate (TPA) for one week and started to receive UV radiation twice a week for 16 weeks. UV dose was titrated up to 300 mJ/cm^2 in order to induce and maintain skin rash in the test group. Skin rash and tumor development were monitored and recorded weekly over the duration of the study.

Tacrolimus treatment protocol

In order to test the effect of systemic immunosuppressive medications on cancer development in the context of lupus-associated inflammation, we employed a skin carcinogenesis protocol described above (Fig. 5A). Briefly, on the first day, four eight-week old female MRL/*lpr* and MRL/*n* control mice were shaved on their back and treated with 50 µg DMBA. The following week, all mice received two doses of 6 µg TPA in one week and started to receive UV radiation (300 mJ/cm^2) twice a week together with intraperitoneal injections of (1mg/kg) of tacrolimus three times per week for 9 weeks. The skin rash and tumor progression was monitored during the course of the experiment.

Flow cytometry

Lymph nodes and back skin of MRL/*lpr* and MRL/*n* control mice were harvested and analyzed using flow cytometry. Lymph nodes were obtained and incubated in collagenase IV (Worthington Biochemical, Lakewood, NJ)-containing digestion buffer for one hour at 37°C. Single cell suspension was obtained by first homogenizing and then filtering the cell suspension

through a 70µm cell strainer. Back skin was harvested and homogenized using the same method. Before staining the cells with fluorochrome-conjugated antibodies, all cells were treated with 2.4G2 supernatant to block Fc receptors. Cells were stained with the following monoclonal surface antibodies: CD3e (145-2C11, eBioscience, San Diego, CA), CD4 (RM4-5, eBioscience), CD8α (53-6.7, eBioscience), CD44 (IM7, eBioscience), and PD-1 (J43, eBioscience). Intracellular stains were performed after fixation and permeabilization with Foxp3/Transcription Factor Staining Buffer Set (eBioscience). Subsequently, all cells were stained with the following antibodies: GATA-3 (TWAJ, eBioscience), Foxp3 (FJK-16s, eBioscience) and T-bet (eBio4B10, eBioscience). Cells were assayed on a FACS Canto flow cytometer (BD Bioscience) and data were analyzed using FlowJo software (Tree Star, Ashland, OR).

Histology, immunohistochemistry and immunofluorescence

Dorsal skin samples were harvested from MRL/*lpr* and MRL/*n* control mice and fixed in 4% paraformaldehyde (PFA) overnight at 4 °C. Subsequently, tissues were dehydrated in ethanol, processed and embedded in paraffin according to standard histology processes. The paraffin-embedded tissues were sectioned at 5 µm, deparaffinized and stained with hematoxylin and eosin (H&E) and toluidine blue (Sigma-Aldrich, St. Louis, MO) to detect mast cells. Masson's trichrome stains (Sigma-Aldrich) were used to stain for scarring according to the manufacturer's protocol. Where indicated, chromogenic staining was performed on tissue sections using Ventana Discovery Ultra staining platform, primary and secondary antibodies are listed in Supplementary Table S1A.

For immunofluorescent staining, the paraffin-embedded tissues were sectioned at 5µm. After deparaffinization, sections were permeabilized in PBS 0.2% Triton X-100 (Thermo Fisher Scientific Inc, Waltham, MA) and antigen retrieval was performed in Vector Lab Antigen Retrieval Solution (Vector Laboratories, Burlingame, CA) by heating the sections for 20 minutes at 95 °C. Nonspecific protein binding was blocked with 5% goat serum (Sigma-Aldrich, St.

Louis, MO) in 5% BSA-PBS before incubation with the anti-mouse antibodies listed in Supplementary Table S1A. DAPI (Thermo Fisher Scientific Inc) nuclear stain was used as counterstain. Histology images were taken using a fluorescence microscope (Zeiss Axio Scan, Oberkochen, Germany).

Quantitative RT-PCR

Dorsal skin samples of MRL/*lpr* and MRL/*n* control mice were harvested, homogenized and lysed in RLT Lysis Solution by making use of a Mini-BeadBeater-8 (BioSpec Products, Inc., Bartlesville, OK). MRL/*lpr* skin was divided into rash and no rash portions. Total RNA from homogenized tissue was isolated using an RNeasy Mini Kit (Qiagen, Netherlands, Venlo, Limburg) and subsequently quantified using a NanoDrop ND-1100 (NanoDrop Technologies). cDNA samples were prepared by using 1µg of total RNA with Invitrogen SuperScript II Reverse Transcriptase (Life Technologies, Carlsbad, CA)**.** Transcription levels of all cDNA samples were assessed by running the samples on a LightCycler® 480 System (Roche Molecular Systems Inc, Pleasanton, CA) with iTaq™ Universal SYBR® Green Supermix (Bio-Rad Laboratories, Hercules, CA) or TaqMan Universal Master Mix II 4440040 (Applied Biosystems). Primer sequences for SYBR green and Taqman analysis are listed in Supplementary Table S1B. Quantitative real-time PCR for SYBR green analyses were performed in a final reaction volume of 10µL consisting of 2µL cDNA of the respective sample and 8µL of SYBR green master mix mixed with the corresponding primers (2µM) for each gene. TaqMan analysis was performed in a final reaction of 10µL consisting of 4.5µL cDNA of the respective sample and 5.5µL of TaqMan master mix mixed with the corresponding primers (20µM) for each gene. All reactions were performed in triplicate and transcription levels were normalized to *GAPDH* levels.

Protein analysis

Skin tissue lysates of MRL/*lpr* and MRL/*n* control mice were collected. For MRL/*lpr* mice, skin was divided into rash and no rash portions. Subsequently, IL-4, IL-6, IL-10, IL-17a, TNFα, TGF-β1 and IFNγ levels were determined using Elisa and BioLegend LEGENDplex™ kits according to the manufacturer's instructions (BioLegend, San Diego, CA).

Supplementary Figures

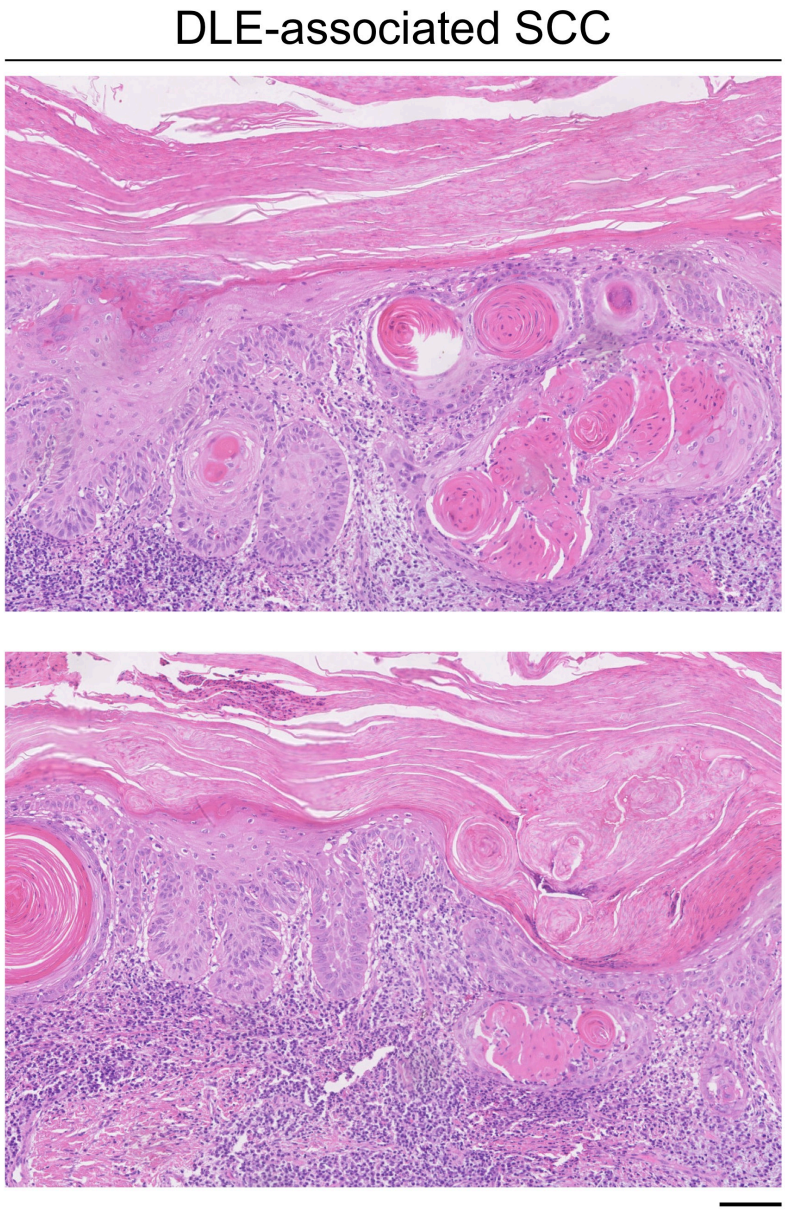

Figure S1. Squamous cell carcinoma in the cancer-prone DLE plaque. H&E images of superficially invasive SCC are shown; scale bars: 100 μm.

Figure S2. Second clinical case of DLE-associated skin cancer. 55-year-old African American patient developed a biopsy-confirmed cancerous lesion (red circle) at the margin of a de-pigmented DLE plaque on her left cheek. H&E, Masson's trichrome for scar detection and CD45 (pan-leukocyte marker) stains of the skin cancer are shown; scale bars: 100 μm.

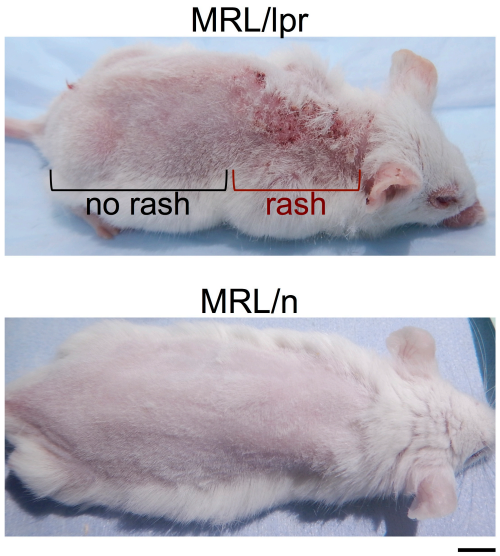

Figure S3. Areas of skin rash and no rash in MRL/*lpr* mice. Representative images of MRL/*lpr* and MRL/*n* mice that are treated with skin carcinogenesis protocol (Fig. 2A) are shown; scale bar: 1 cm.

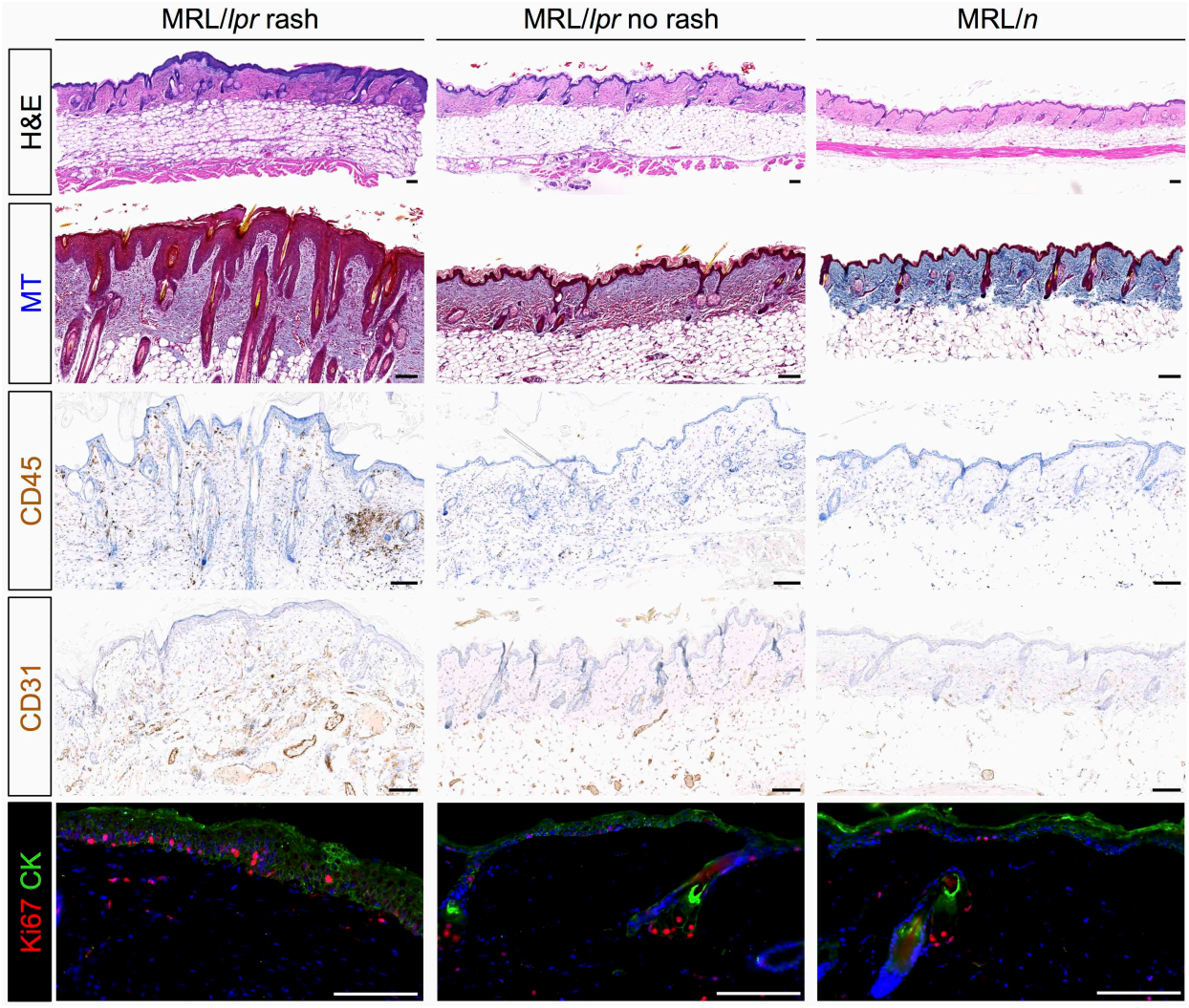

Figure S4. MRL/*lpr* skin rash is marked by accumulation of leukocytes, expansion of blood vessels and epidermal hyperplasia without scarring. Representative images of H&E, Masson's trichrome (MT), CD45 (pan-leukocyte marker), CD31 (endothelial marker) and Ki67/cytokeratin (CK)-stained skin sections of MRL/*lpr* (rash and no rash) and MRL/*n* are shown. Note the dense leukocyte infiltrate in the dermis accompanied by increased keratinocyte proliferation and epidermal thickening in MRL/*lpr* skin rash; scale bars: 100 μm.

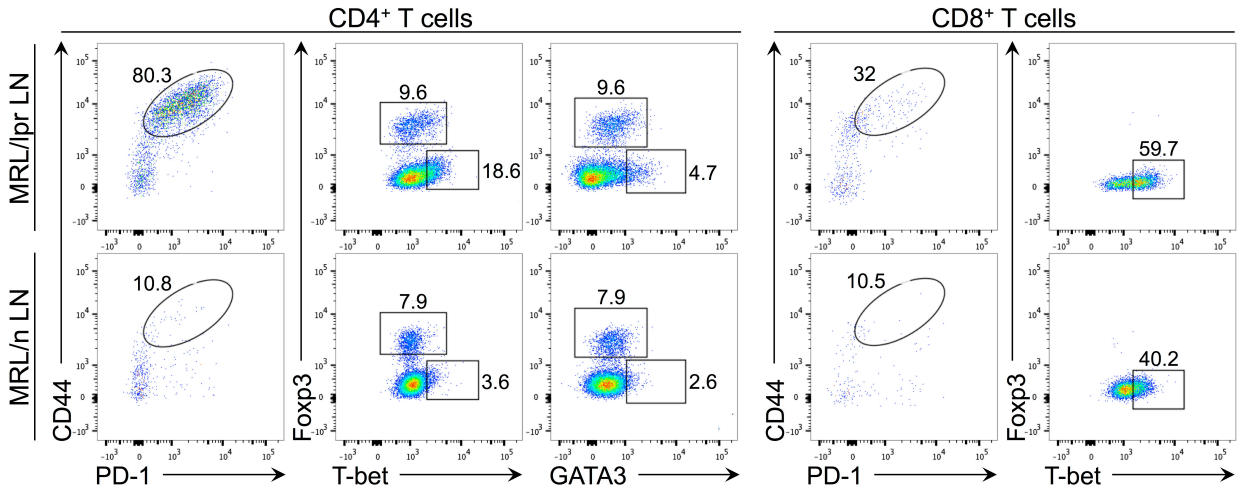

Figure S5. Degree of T cell activation and its subtypes in the lymph nodes of lupus-prone mice. Representative flow analysis of MRL/*lpr* and MRL/*n* lymph nodes demonstrates the percentage of $CD44^+$ $PD1^+$ activated $CD4^+$ and $CD8^+$ T cells, $Foxp3^+$ Tregs, T-bet^+ Th1 and $GATA3^+$ Th2 cells.

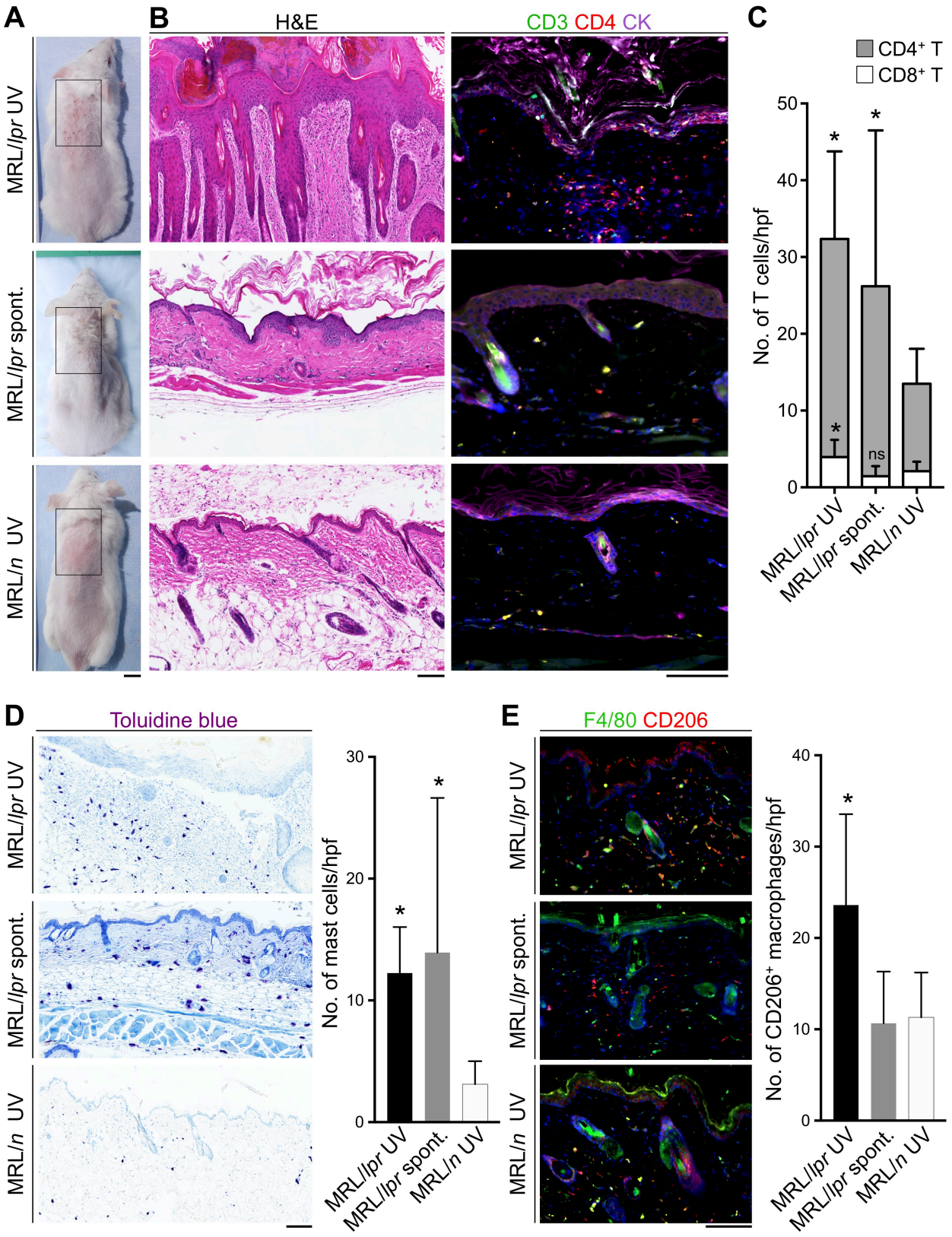
A
B
H&E
CD3 CD4 CK
C
CD4⁺ T
CD8⁺ T
MRL/lpr UV
MRL/lpr spont.
MRL/n UV
No. of T cells/hpf
50
40
30
20
10
0
*
ns
D
Toluidine blue
No. of mast cells/hpf
30
20
10
0
E
F4/80 CD206
No. of CD206⁺ macrophages/hpf
40
30
20
10
0

Figure S6. Immune environment of spontaneous and UV-induced cutaneous lupus in MRL/*lpr* mice. (**A**) Representative images of UV-treated MRL/*lpr* and MRL/*n* control mice (age: 4 months) and MRL/*lpr* mouse with spontaneous rash (spont.; age: 7 months) are shown. Boxes highlight the skin regions used for histological analysis. (**B**) Representative H&E and immunostaining images of the skin demonstrate the degree of epidermal hyperplasia, skin inflammation and $CD4^+$ T cell infiltrate in UV-treated and spontaneous MRL/*lpr rash* and MRL/*n* skin (CK: cytokeratin). (**C**) T cell infiltrates in UV-treated and spontaneous MRL/*lpr* rash and MRL/*n* control skin are quantified by counting the number of cells in 10 random high power fields (hpf) per skin section and averaging the counts across the animals in each group. (**D**) Mast cells are shown in representative images of toluidine blue-stained UV-treated and spontaneous MRL/*lpr* rash and MRL/*n* control skin and quantified in 10 random hpf per skin section across the animals in each group. (**E**) Representative images show $CD206^+$ $F4/80^+$ M2 macrophages in UV-treated and spontaneous MRL/*lpr* rash and MRL/*n* control skin and the bar graph demonstrates the average number of macrophages in 10 random hpf per skin section across the animals in the study groups. n = 3 per group; stained cells were counted blindly; $*p < 0.05$; compared to UV-treated MRL/*n* control skin by Student's *t* test; scale bars: 100 μm.

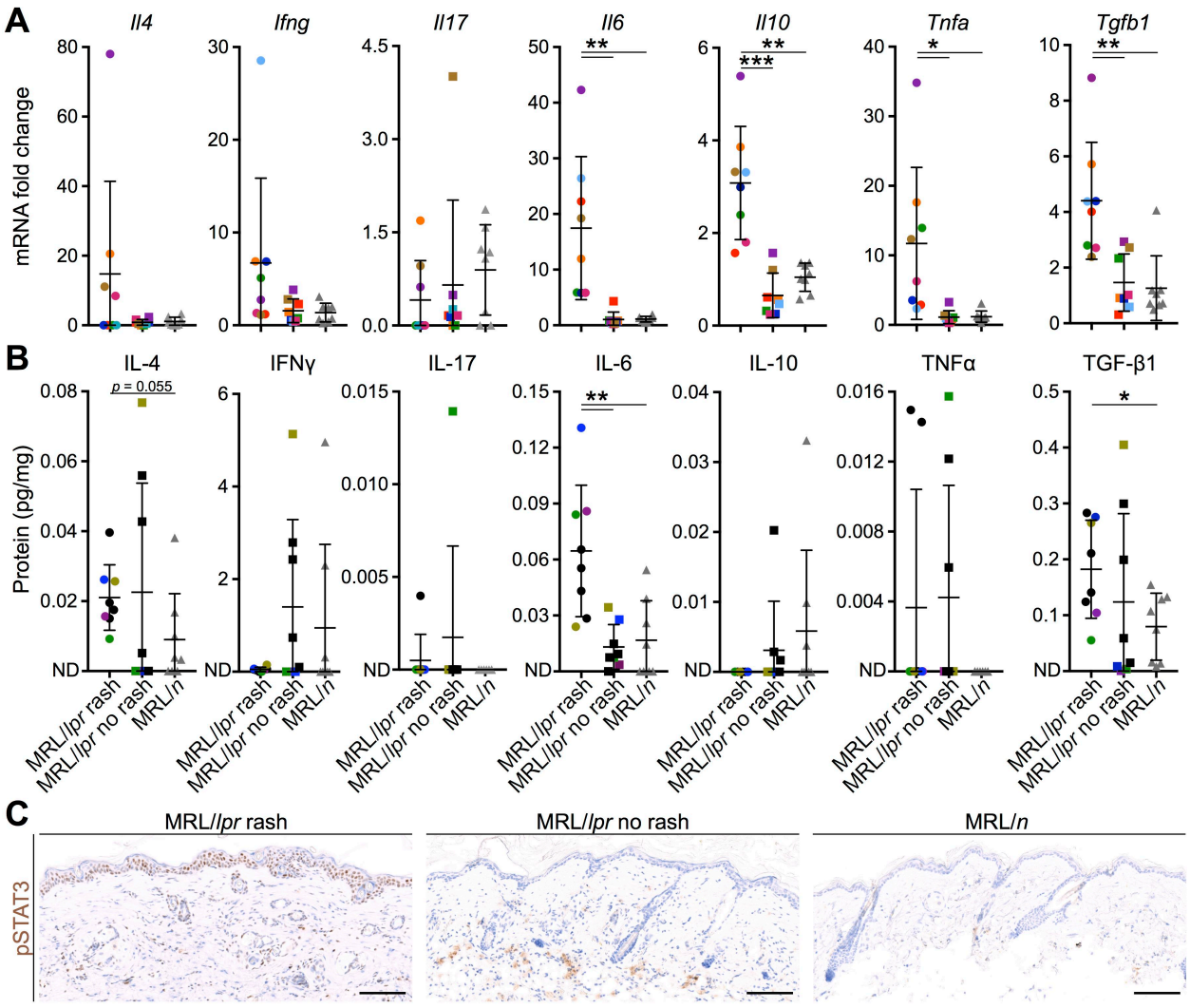

Figure S7. Pro-tumorigenic cytokines are upregulated in MRL/*lpr* skin rash. (**A, B**) Gene expression (**A**) and protein levels (**B**) of cytokines associated with T helper polarization and pro-inflammatory cytokines are measured in MRL/*lpr* rash, no rash and MRL/*n* skin. Note IL-4 protein level shows a trend towards upregulation in MRL/*lpr* rash (p = 0.055). Color-coded points highlight the rash and no rash skin samples from the same MRL/*lpr* mouse (ND: not detectable). (**C**) pSTAT3 nuclear stain in representative images demonstrate the degree of IL-6 signaling onto keratinocytes in MRL/*lpr* rash, no rash and MRL/*n* control skin. n = 8 per group; *p < 0.05; **p < 0.01; ***p < 0.001 by Student's t test; scale bars: 100 μm.

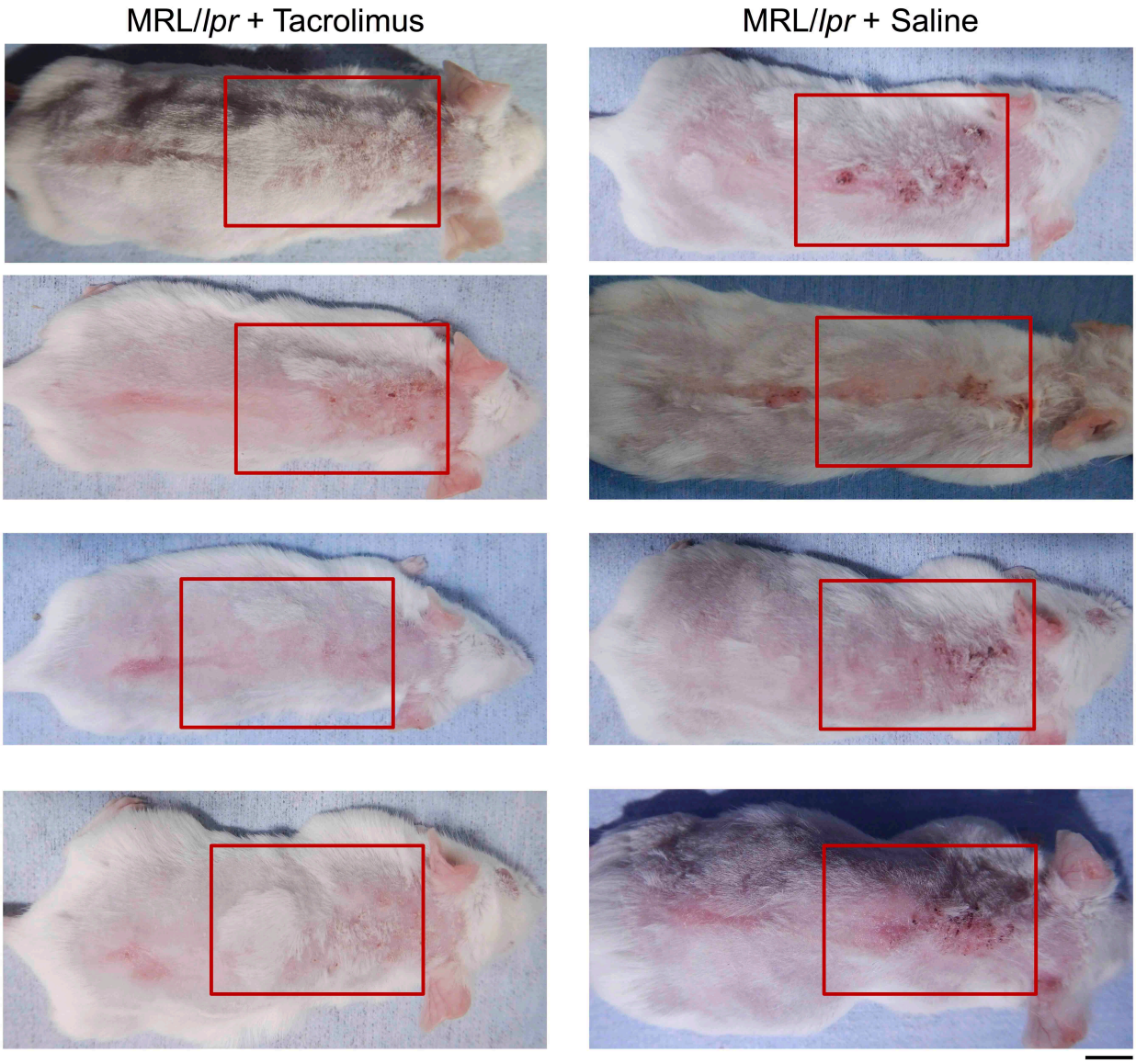

Figure S8. Tacrolimus treatment suppresses cutaneous lupus inflammation in MRL/*lpr* mice. Images of MRL/*lpr* mice treated with tacrolimus and MRL/*lpr* mice treated with saline during skin carcinogenesis protocol are shown. Red boxes highlight the skin areas that are prone to cutaneous lupus rash development in MRL/*lpr* mice (scale bar: 1cm).

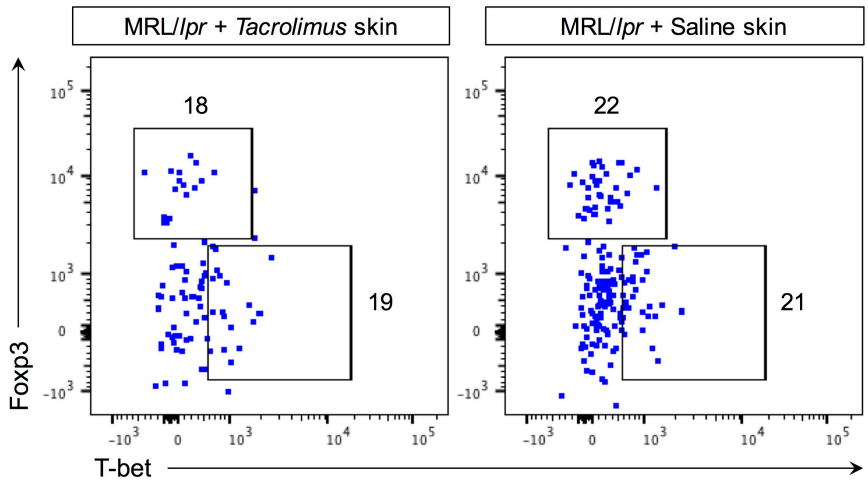

Figure S9. Treg cells are reduced in the skin of MRL/*lpr* mice treated with tacrolimus. Representative flow analysis and the average percentage of Foxp3$^+$ (Treg) and T-bet$^+$ (Th1) of CD4$^+$ T cells isolated from the upper back skin of MRL/*lpr* mice treated with tacrolimus or saline (control) are shown.

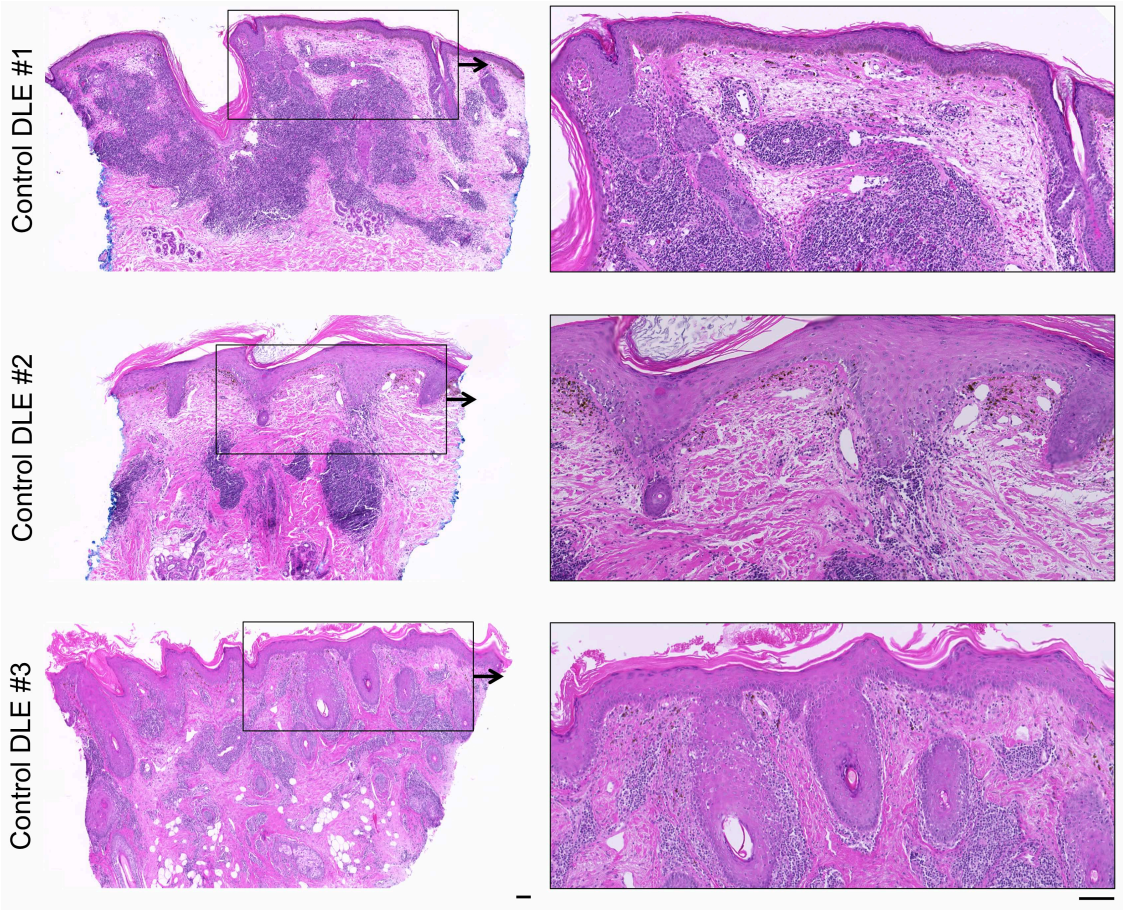

Figure S10. DLE lesion biopsies from three African American patients with no history of skin cancer. H&E of the punch biopsy specimen are shown; scale bars: 100 μm.

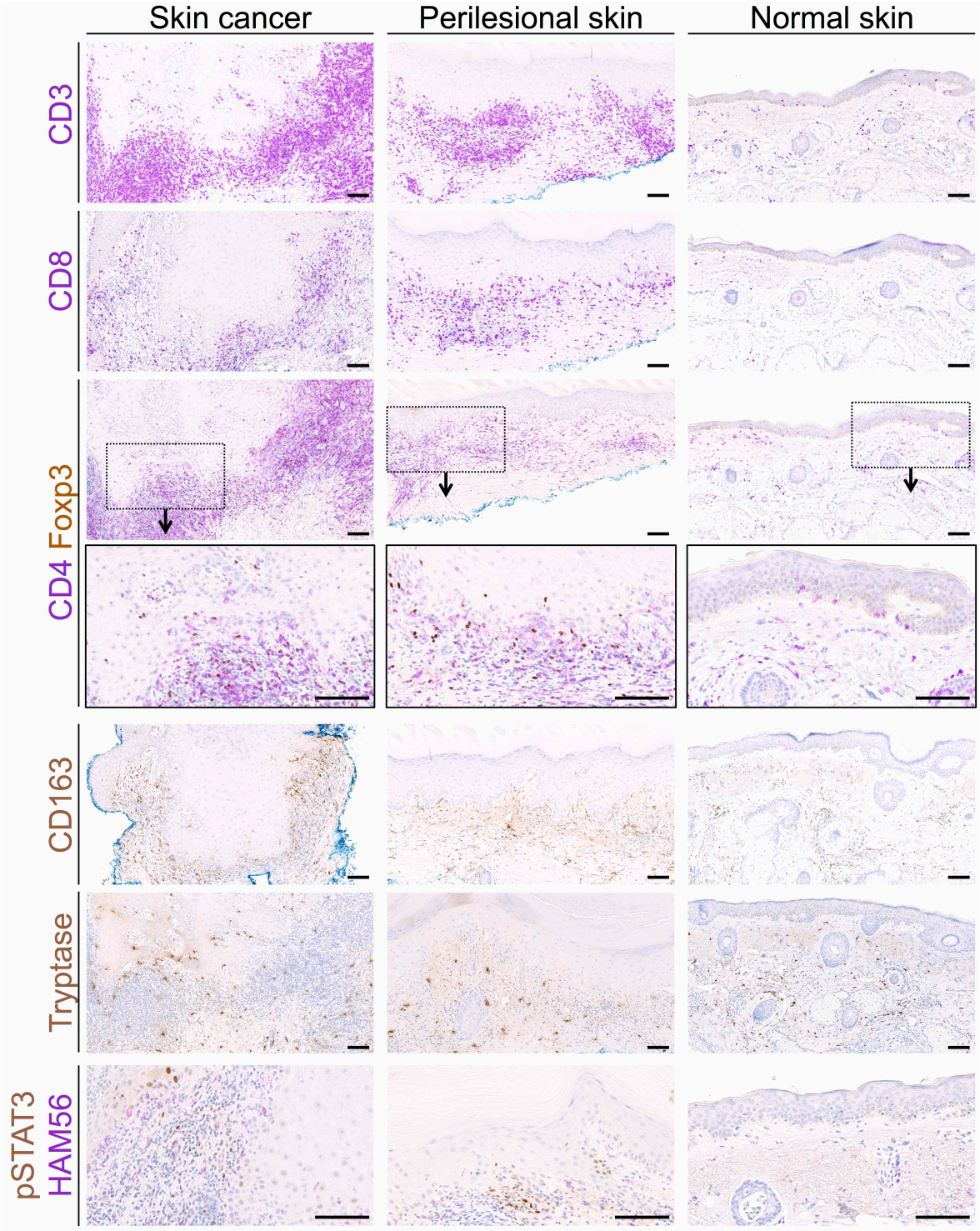

Figure S11. Tumor-promoting immune milieu around the skin cancer site in second DLE patient. Immunostaining demonstrates the accumulation of T cells including Foxp3^{+} Tregs,

$CD163^+$ M2 macrophages and $tryptase^+$ mast cells in DLE-associated skin cancer and the perilesional skin compared to age-matched normal facial skin. pSTAT3 staining shows the keratinocyte with activated STAT3 signaling. HAM56 stains the dermal macrophages; scale bars: 100 μm.

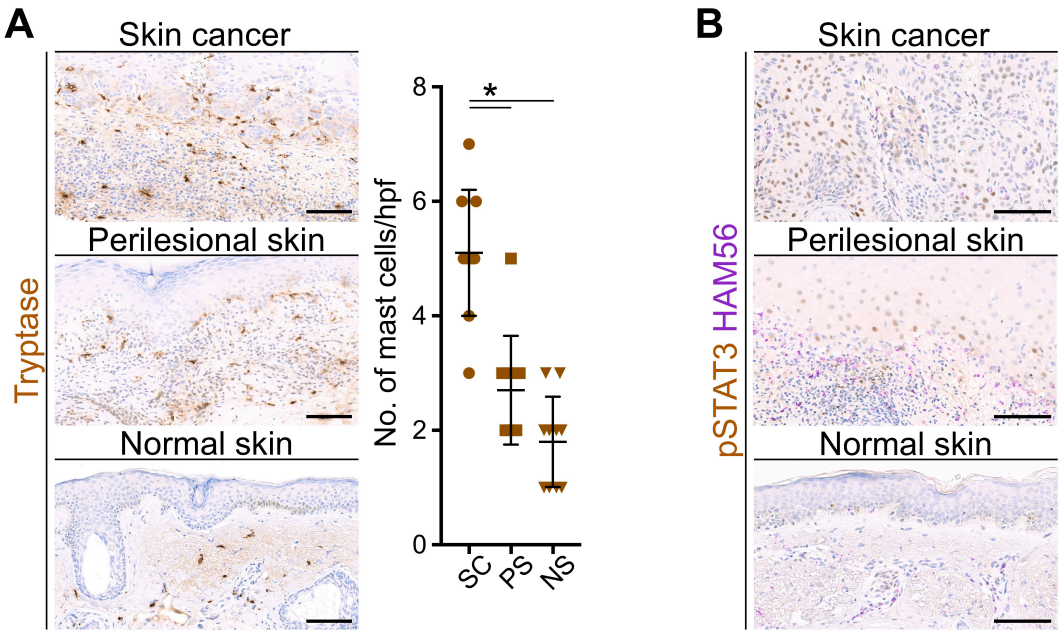

Figure S12. Cancer-prone DLE plaque is marked by mast cell infiltrate surrounding the sites of skin cancer development and STAT3 signaling in the perilesional skin. (**A**) Tryptase-positive mast cells are stained and quantified in the skin cancer, perilesional skin of DLE and normal skin. Representative images and cell quantification in 10 random hpf views are shown. (**B**) pSTAT3 staining highlights STAT3 signaling activity in the keratinocytes of the skin cancer, perilesional skin of DLE and normal skin. HAM56 stains the dermal macrophages. Stained cells were counted blindly; *$p < 0.001$ by Student's *t* test; scale bars: 100 μm.

Table S1. Antibodies and primers used for tissue analysis.

A

Primary Antibodies	Clone	Company
Rabbit Anti-Human CD3	2GV6	Ventana Medical Systems
Rabbit Anti-Human CD4	SP35	Ventana Medical Systems
Rabbit Anti-Human CD8	SD37	Ventana Medical Systems
Mouse Anti-Human CD163	10D6	Leica Biosystems, Buffalo Grove, IL
Rabbit Anti-Human Foxp3	D2W8E	Cell Signaling Technology, Danvers, MA
Mouse Anti-Human Macrophage	HAM56	Ventana Medical Systems
Rabbit Anti-pStat3 (Tyr705)	D3A7	Cell Signaling Technology, Danvers, MA
Tryptase	AA1	DAKO, Santa Clara, CA
Rabbit Anti-Mouse CD3	Polyclonal	Abcam, Cambridge, MA
Rabbit Anti-Mouse CD4	EPR19514	Abcam, Cambridge, MA
Mouse Anti-Mouse Cytokeratin	AE1/AE3	Agilent, Santa Clara, CA
Rat Anti-Mouse CD31	Polyclonal	BioLegend, San Diego, CA
Rabbit Anti-Mouse Ki67	Polyclonal	BioLegend, San Diego, CA
Rat Anti-Mouse F4/80	BM8	Biolegend, San Diego, CA
Rat Anti-mouse CD206	C068C2	BioLegend, San Diego, CA
Rat Anti-Mouse CD45	30-F11	BioLegend, San Diego, CA
Secondary Antibodies and staining kits		
Goat anti-Mouse IgG, Alexa Fluor® 488 conjugate		Thermo Fisher Scientific
Goat anti-Rabbit IgG, Alexa Fluor® 568 conjugate		Thermo Fisher Scientific
Goat anti-Mouse IgG, Alexa Fluor® 647 conjugate		Thermo Fisher Scientific
UltraView Universal DAB Detection Kit	760-500	Ventana Medical Systems
Omni Map anti-Rabbit - HRP	760 - 4311	Ventana Medical Systems
Omni Map anti-Mouse - HRP	760 - 4310	Ventana Medical Systems
Discovery Purple Kit	760 - 229	Ventana Medical Systems
Discovery DAB Kit	760 - 159	Ventana Medical Systems
Chemical for Special Stains		
Toluidine Blue		Sigma, St. Louis, MO
Masson's trichrome		Sigma, St. Louis, MO

B

Gene Name	Forward Primer	Reverse Primer
IL-6	TCTTCAGTATGTCTAGCCCCTG	AGGCGCCCAACTGTGCTAT
IL-10	GCTCTTACTGACTGGCATGAG	CGCAGCTCTAGGAGCATGTG
IFNy	ATGAACGCTACACACTGCATC	CCATCCTTTTGCCAGTTCCTC
TNFa	CCCTCACACTCAGATCATCTTCT	GCTACGACGTGGGCTACAG
TGFb1	GCTGAACCAAGGAGACGGAAT	CAAGAGCAGTGAGCGCTGAA

Taqman	Prime Time Assays (Integrated DNA Technologies, Coraville, IO)	
	Custom Probe	**Exon Location**
IL-4	Mm.PT.28.32703659	4-5
IL-17	Mm.PT.58.6531092	2-3